Dynamic Martian magnetosphere: Transient twist induced by a rotation of the IMF

Ronan Modolo, Gérard Chanteur, Eduard Dubinin

Dynamic Martian magnetosphere: Transient twist induced by a rotation of the IMF

R. Modolo,[1] G. M. Chanteur,[2] and E. Dubinin[3]

Received 4 October 2011; revised 2 December 2011; accepted 7 December 2011; published 11 January 2012.

[1] Simulation studies of the Martian environment are usually restricted to stationary situations under various steady conditions of the solar wind and solar radiation. Dynamic transients and their implications have so far attracted little attention although global simulation models can provide valuable insights to understand disagreements between simulations and in situ observations. We make use of a three dimensional multispecies hybrid simulation model to investigate the response of the Martian plasma environment to a sudden rotation of the IMF. The simulation model couples charged and neutral species via three ionisation mechanisms: the absorption of solar extreme ultraviolet radiation, the impact of solar wind electrons, and the charge exchange between ions and neutral atoms. When a rotational discontinuity conveyed by the solar wind reaches the Martian environment the bow shock adapts quickly to the new solar wind conditions in contrast to the induced magnetosphere, especially the magnetic lobes in the wake. Timescales necessary to recover a stationary state can be estimated from such simulations and have some implications for space observations especially in the use of magnetic field proxies and for organizing particle measurements made by a spacecraft like Mars Express without an onboard magnetometer. **Citation:** Modolo, R., G. M. Chanteur, and E. Dubinin (2012), Dynamic Martian magnetosphere: Transient twist induced by a rotation of the IMF, *Geophys. Res. Lett.*, *39*, L01106, doi:10.1029/2011GL049895.

1. Introduction

[2] The Martian ionized environment has been explored since a few decades by several space missions: Mariner 6, Phobos-2, Mars Global Surveyor, Mars Express to mention only a few. Observations have stressed a very complex and extremely dynamic environment. Long and short term variations of the solar wind (bulk speed, density, orientation and magnitude of the interplanetary magnetic field (IMF) ..) can alter the plasma environment of the planet [*Edberg et al.*, 2009]. For instance, the impact of a dense and high pressure solar wind (Corotating Interaction Regions, CIRs) can strongly affect the Martian plasma environment, leading to large perturbations of its induced magetosphere and its ionosphere [*Dubinin et al.*, 2009; *Edberg et al.*, 2010]. However, it is usually difficult to distinguish between spatial and temporal variations from observations made by a single spacecraft. In this context, global simulations allow to set back in situ observations into a global frame. Physical parameters specifying the IMF, the solar wind plasma, and the radiation spectrum in the UV and EUV ranges are kept constant during the course of most simulations which usually converge toward a stationary state after some computational transient due to the lack of consistency between the initial state of the simulation and the selected parameters. A given simulation can be restarted without computational transient from an achieved stationary state for which exhaustive data have been saved. Physical parameters could subsequently be changed in order to model some naturally evolving situation. The goal of this study is to describe the response of the Martian plasma environment to a rotation of the IMF and identify characteristic timescales of this response. Similar attempts have been done in studies of Titan environment to support and help the comprehension of Cassini observations during a Saturn's magnetopause crossing by Titan [*Bertucci et al.*, 2008; *Ma et al.*, 2009; *Simon et al.*, 2009]. The simulation model and parameters used for this study are detailed in section 2. Times scales required to recover a stationary state for the Bow Shock, the Induced Magnetospheric Boundary (IMB)/Magnetic Pile-up Boundary (MPB), the magnetic lobes and the planetary plasma are discussed in sections 3.1–3.4.

2. Simulation Model

[3] Several numerical models have been developed, within different frameworks such as MHD, multifluid or hybrid, in order to characterize the solar wind interaction with the Martian upper atmosphere [e.g., *Brain et al.*, 2010]. The model used in this study adopts the so-called hybrid formalism where a fully kinetic description is applied to ions meanwhile electrons are treated as a massless fluid which ensures the charge neutrality of the plasma and contributes to the total current and pressure. Plasma - neutral interactions are described in a self-consistent way from a local calculation of production rates of the different ionisation mechanism of the upper atmosphere (photoionisation, electronic impact and charge exchange). This model has been used to describe the Martian environment at maximum and minimum solar activity [*Modolo et al.*, 2005, 2006].

[4] To study the effect of a rotation of the IMF, a simulation is performed with a realistic set of solar wind plasma parameters. The density of solar wind ions is fixed to 1.25 cm^{-3}, their temperature to 10 eV, the bulk solar wind speed to 550 km/s and the IMF to 2.5 nT aligned with the Parker spiral leading to an angle of 57° between the IMF and the solar wind flow direction. Parameters chosen for the solar EUV flux and the Martian neutral corona are relevant to

[1]UVSQ/LATMOS-IPSL/CNRS-INSU, Guyancourt, France.
[2]LPP-Ecole Polytechnique, Vélizy, France.
[3]MPS, Lindau-Katlenburg, Germany.

0094-8276/12/2011GL049895

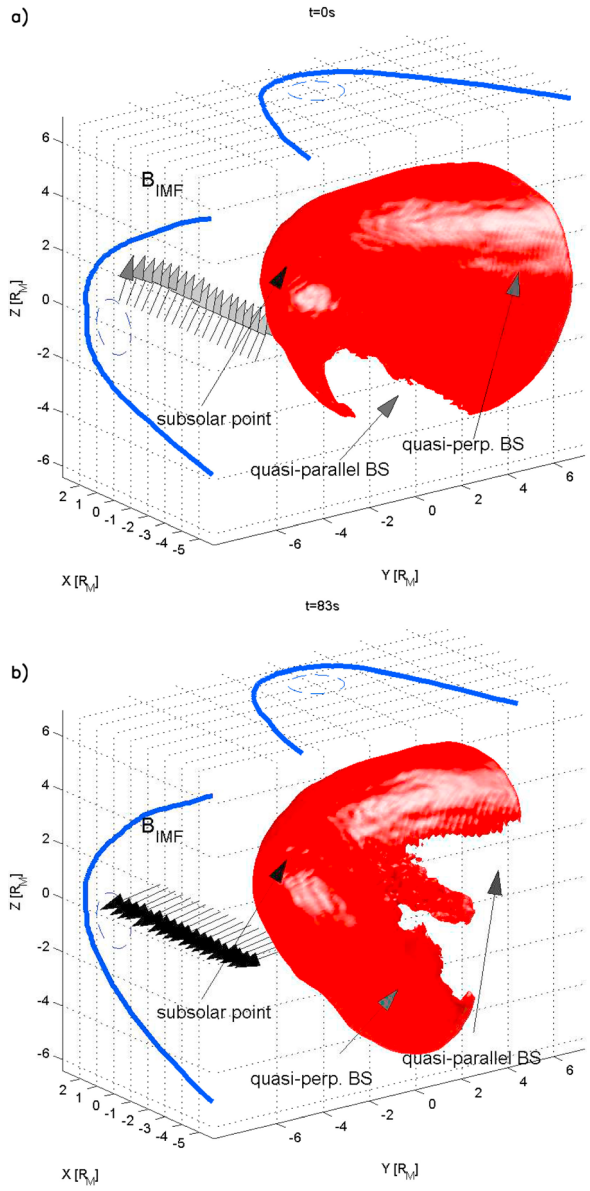

Figure 1. Visualisation of the BS location with an isovalue surface of the magnetic field. (a) The BS location at t = 0 s with the "old" IMF and (b) the BS location in the "new" IMF configuration (at t = 83 s). The parallel BS region is identified by a lower magnitude of the magnetic field leading to the teared off part of the paraboloid like surface of the BS. The orientation of the IMF in the undisturbed solar wind is shown with black arrows. Projections of the BS in XY and XZ planes are displayed in blue thick lines while the projection of the planet is in dashed blue line.

conditions of maximum solar activity. The density profile of atomic hydrogen is given by the simplified Chamberlain's expression. The density and the temperature at the exobase are the key parameters which govern the density profile and we have adopted the values given by *Krasnopolsky* [1993]. Oxygen profile density is derived from Monte Carlo simulation computed by *Kim et al.* [1998], for the supra-thermal oxygen population, and from the atmospheric model for cold oxygen atoms [*Krasnopolsky and Gladstone*, 1996]. Photoionization frequencies are equal to 3.1×10^{-7} s^{-1} for oxygen and 4.2×10^{-8} s^{-1} for hydrogen. The simulation is performed in a cartesian simulation box in the Mars-centered Solar Orbital (MSO) coordinate system: the X-axis points from Mars toward the Sun, the Y-axis is anti-parallel to Mars' orbital velocity vector and the Z-axis completes the right handed system. The size of the box ranges from -6 R_M to 3 R_M for X_{MSO}, and from -11 R_M to 11 R_M for Y_{MSO} and Z_{MSO} with a spatial resolution of about 300 km.

[5] As a first step, the simulation is performed with the IMF in the $(XZ)_{MSO}$ plane (hereafter named old IMF) until a quasi-stationary solution is reached after about 900 s. A clockwise rotation of the IMF at 90° around the X_{MSO} axis is operated on the entry face of the simulation box (at X_{MSO} = 3 R_M) as shown in Figure 1a. The imposed rotation of the IMF defined by $\theta(t) = \pi/4 + \frac{1}{2}\arctan((10 - t)/4)$ lasts 20 s and is consistent with observed timescales for such IMF changes. After completion of this rotation, the IMF (hereafter named new IMF) is in the $(XY)_{MSO}$ plane. This time dependent boundary condition imposed on the entry face of the simulation domain creates a rotational discontinuity with a finite width affecting the different boundaries and plasma regions of the induced magnetosphere as it is convected by the solar wind through the simulation domain.

3. Simulation Results

[6] The Martian environment adapts to the new IMF configuration with several timescales according to the different boundaries and regions (Bow Shock, Induced Magnetic Boundary, magnetic lobes) and these timescales are different for the field and the particles. These different timescales are detailed in this section.

3.1. Response of the Bow Shock

[7] With an IMF in the $(XZ)_{MSO}$ plane before the rotation (with $B_z > 0$), a parallel Bow Shock (BS) region (region of the BS where the shock normal is parallel to the IMF direction) can be identified in the -Z half plane. Figure 1 represents an isovalue surface of the total magnetic field at 5 nT highlighting the BS surface at t = 0 s corresponding to the old IMF and at t = 83 s corresponding to the new IMF configuration, once the transient twist has crossed the whole simulation box. The quasi-parallel BS can be easily identified by a hole on the isovalue surface due to the absence of magnetic field jump between upstream and downstream region through the quasi-parallel BS. Part of the southern magnetic lobe of the induced magnetosphere is seen from this hole corresponding to the parallel BS. Following the IMF rotation, indicated by the black arrows in Figure 1, this parallel BS region is progressively shifted to the +Y half plane. The magnetic flux tubes embedded into the solar wind plasma are transported with the solar wind speed and the BS being located in this plasma is almost instantaneously adapted to the new configuration of the IMF. Hence at a given time the part of the BS located downstream of the rotational layer, with respect to solar wind flow, corresponds to the old IMF and the upstream part to the new IMF meanwhile the part covered by the rotational layer corresponds to the transition between the old and new IMF. A given point in the MSO frame, located slightly upstream of

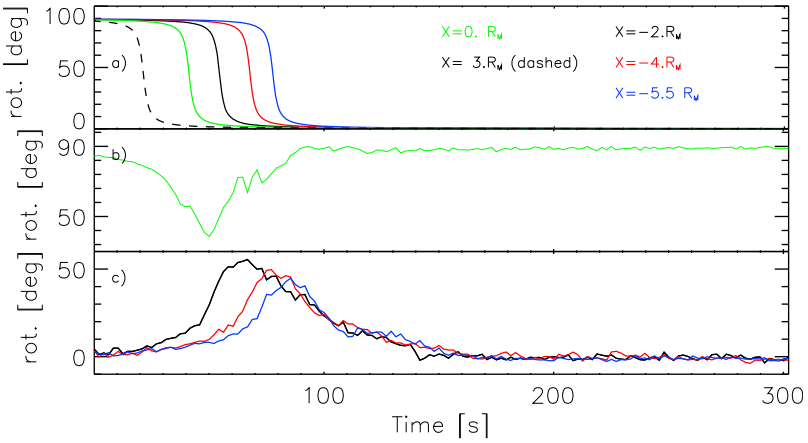

Figure 2. (a) The angle between the IMF in the undisturbed solar wind region and the Z axis for different X locations in the Martian wake and at the entry face of the simulation (dashed line). The rotation takes place at different time for the considered X values, emphasizing the propagation of the rotation. (b) The angle between the IMF in the undisturbed region and the magnetic equator defined in the terminator plane (X = 0 R_M). (c) The shift angle of the magnetic lobes defined as the angle between the vector defined by the barycenters of the lobes, from southern to northern lobe, and the IMF at the same abscissa.

the BS could be successively upstream of the perpendicular shock, then of the parallel shock and eventually upstream of the perpendicular shock.

3.2. Response of the MPB

[8] The MPB is produced and identified by the pile-up of the magnetic field upstream of the obstacle and separates, roughly, the solar wind from the planetary plasmas. This boundary is asymmetric, according to kinetic simulations [e.g., *Bößwetter*, 2004; *Modolo et al.*, 2006; *Kallio et al.*, 2010], and the magnetic field pile-up is stronger in the hemisphere where the motional electric field is pointing outward from this boundary ($\vec{E}_{conv} = -\vec{V} \times \vec{B}$) while in the opposite hemisphere, no evidence of magnetic field increase is seen. In the terminator plane the MPB is symmetric with respect to the magnetic equator (Bx $\sim$ 0 in the draping region). The recovery time of the MPB can be obtained by tracking the angle between the IMF vector in the solar wind region and the symmetry axis of the MPB, which coincides approximately with the magnetic equator, in the terminator plane. Figure 2a indicates the rotation of the IMF in the undisturbed solar wind region at different X values while Figure 2b shows the angle between the IMF in the solar wind and the symmetry axis of the MPB in the terminator plane. A 90° angle indicates that the magnetic equator is perpendicular to the IMF, as expected in a stationary state, while a 0° angle means that the magnetic equator is parallel to the IMF. This boundary needs a few tens of seconds (about 60s) to adapt to the new configuration of the magnetic field lines as it can be seen in Figure 2b. This result is very likely from the combination of two factors. On one hand, some time is required to the new magnetic flux tubes to form the new MPB and on the other hand the older piled-up magnetic flux tubes, corresponding to the previous IMF configuration, are evacuated with a convection time larger than the one in the solar wind region due to the presence of the dense and cold ionospheric plasma. Due to a poor representation of the Martian ionosphere in our model, magnetic field lines might require larger time to penetrate in the deepest part of the ionosphere. The present model is not suited to investigate this particular region and needs to be completed with a ionospheric model taking into account the main chemical reactions and the electrical conductivities.

3.3. Response of the Magnetic Lobes

[9] In response to the draped field lines around the obstacle, a bipolar magnetic tail is formed in the Martian plasma wake. These lobes are located above and below the magnetic equator, i.e. for the old IMF the XZ plane passing through the center of the planet, and the XY plane for the new IMF. The adaptation time of the lobes to the new IMF configuration can be deduced from Figure 2c. A zero angle indicates that the magnetic lobe orientation is in agreement with the expected orientation for a given IMF. A large angle underlines that magnetic lobes are mostly orientated according to the old IMF. Figure 2c shows that, following the IMF rotation, magnetic lobes configuration are consistent with the new IMF orientation after about one hundred seconds. It also provides a recovering time of the magnetic lobes at different distances in the wake and reveal that lobes farther in the wake start rotating before the new IMF orientation reaches the given position in the undisturbed solar wind region and have a smaller twist with respect to the IMF than lobes closer to the planet.

3.4. Response of the Planetary Plasma

[10] Many hybrid simulations have emphasized two main escape channels for heavy planetary ions such as O^+, a first one in the Martian wake with relatively large densities in the plasma sheet and a second one with a plume-like shape in the direction of the motional electric field [e.g., *Brain et al.*, 2010]. Such features have also been observed with Mars-Express (MeX) measurements [*Barabash et al.*, 2007]. A response of escape fluxes to the IMF changes can be determined from Figure 3. Density maps of O^+ ions in the $(YZ)_{MSO}$ plane at X = $-4R_M$ are presented for several times corresponding to different stages of the IMF orientation (t = 0, 62, 83, 125 s). A t = 0 s, the IMF is aligned with the

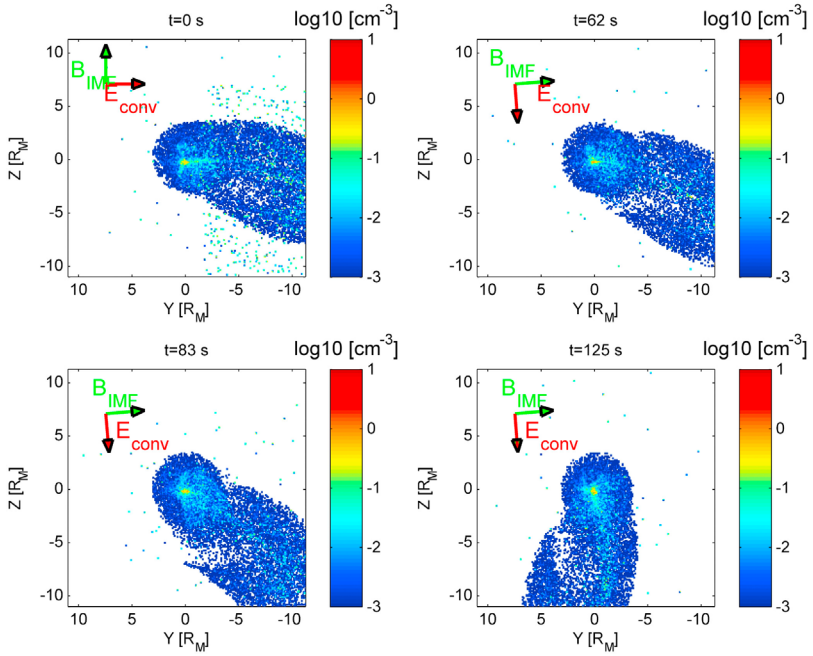

Figure 3. Density maps of O^+ ions in the Martian wake at X = 4 R_M for different simulation time. The orientation of the magnetic and motional electric fields are displayed by red and green arrows.

+Z direction and the E_{conv} field points in the +Y direction. The largest density is seen in the plasma sheet and an asymmetric plume-like feature is clearly seen in the E_{conv} direction. At t = 62 s, the IMF has already reached its final orientation while the density map of O^+ shows a similar pattern to the map at t = 0 s . Particles are not yet affected by the new IMF orientation. At t = 125 s, the density map of O^+ is consistent with the new IMF orientation. Therefore, ion plume needs between 1–2 min to adapt to the new IMF direction.

4. Conclusion

[11] The BS adjusts almost instantaneously to the new IMF orientation while the MPB and the magnetic lobes require up to 1–2 min, indicating nevertheless a quick adjustment to the new solar wind conditions. This information emphasizes the special care that one have to stress during multispacecraft observation conjunctions such MGS/MeX, MeX/Rosetta or possibly with MeX/MAVEN. Since ion-escape flux are organised by the motional electric field, the computation of the ion escape flux is sensitive to the electric field direction proxy used. Simulations suggest that the ion plume adapts to the new E_{conv} field configuration in about 2 min. A solar wind monitor at Martian orbit or simultaneous measurements in the solar wind region and the Martian environment would be helpful to investigate the dynamics of the induced magnetosphere and its response to different drivers.

[12] **Acknowledgments.** G.M.C., E.D. and R.M. are strongly indebted to the International Space Science Institute (ISSI) for the support given to the International Teams "Comparative Study of Induced Magnetosphere" and "Intercomparison of global models and measurement of the Martian plasma environment". G.M.C. and R.M. are also indebted to the Soleil-Heliosphere-Magnetospheres program of the French Space Agency CNES for its support. Research at LATMOS has been partly supported by ANR-CNRS through contract ANR-09-BLAN-223.E.D. also wishes to acknowledge the DLR for supporting grant FKZ 50 QM 0801 and SPP 1488 W0910/3-1.

[13] The Editor thanks Niklas Edberg and Ying Juan Ma for their assistance in evaluating this paper.

References

Barabash, S., A. Fedorov, R. Lundin, and J. A. Sauvaud (2007), Martian atmospheric erosion rates, *Science*, *315*, 501–503, doi:10.1126/science.1134358.

Bertucci, C., et al. (2008), The magnetic memory of Titan's ionized atmosphere, *Science*, *321*, 1475–1478, doi:10.1126/science.1159780.

Bößwetter, A., T. Bagdonat, U. Motschmann, and K. Sauer (2004), Plasma boundaries at Mars: A 3-D simulation study, *Ann. Geophys.*, *22*, 4363–4379, doi:10.5194/angeo-22-4363-2004.

Brain, D., et al. (2010), A comparison of global models for the solar wind interaction with Mars, *Icarus*, *206*, 139–151, doi:10.1016/j.icarus.2009.06.030.

Dubinin, E., M. Fraenz, J. Woch, F. Duru, D. Gurnett, R. Modolo, S. Barabash, and R. Lundin (2009), Ionospheric storms on Mars: Impact of the corotating interaction region, *Geophys. Res. Lett.*, *36*, L01105, doi:10.1029/2008GL036559.

Edberg, N. J. T., D. A. Brain, M. Lester, S. W. H. Cowley, R. Modolo, M. Fränz, and S. Barabash (2009), Plasma boundary variability at Mars as observed by Mars Global Surveyor and Mars Express, *Ann. Geophys.*, *27*, 3537–3550, doi:10.5194/angeo-27-3537-2009.

Edberg, N. J. T., H. Nilsson, A. O. Williams, M. Lester, S. E. Milan, S. W. H. Cowley, M. Fränz, S. Barabash, and Y. Futaana (2010), Pumping out the atmosphere of Mars through solar wind pressure pulses, *Geophys. Res. Lett.*, *370*, L03107, doi:10.1029/2009GL041814.

Kallio, E., K. Liu, R. Jarvinen, V. Pohjola, and P. Janhunen (2010), Oxygen ion escape at Mars in a hybrid model: High energy and low energy ions, *Icarus*, *206*, 152–163, doi:10.1016/j.icarus.2009.05.015.

Kim, J., A. F. Nagy, J. L. Fox, and T. E. Cravens (1998), Solar cycle variability of hot oxygen atoms at Mars, *J. Geophys. Res.*, *103*(12), 29,339–29,342.

Krasnopolsky, V. A. (1993), Solar cycle variations of the hydrogen escape rate and the CO mixing ratio on Mars, *Icarus*, *101*, 33–41.

Krasnopolsky, V. A., and G. R. Gladstone (1996), Helium on Mars: EUVE and PHOBOS data and implications for Mars' evolution, *J. Geophys. Res.*, *101*, 15,765–15,772, doi:10.1029/96JA01080.

Ma, Y. J., et al. (2009), Time-dependent global MHD simulations of Cassini T32 flyby: From magnetosphere to magnetosheath, *J. Geophys. Res.*, *114*, A03204, doi:10.1029/2008JA013676.

Modolo, R., G. M. Chanteur, E. Dubinin, and A. P. Matthews (2005), Influence of the solar EUV flux on the Martian plasma environment, *Ann. Geophys.*, *23*, 433–444, doi:10.5194/angeo-23-433-2005.

Modolo, R., G. M. Chanteur, E. Dubinin, and A. P. Matthews (2006), Simulated solar wind plasma interaction with the Martian exosphere: Influence of the solar EUV flux on the bow shock and the magnetic pile-up boundary, *Ann. Geophys.*, *24*, 3403–3410, doi:10.5194/angeo-24-3403-2006.

Simon, S., U. Motschmann, G. Kleindienst, J. Saur, C. L. Bertucci, M. K. Dougherty, C. S. Arridge, and A. J. Coates (2009), Titan's plasma environment during a magnetosheath excursion: Real-time scenarios for Cassini's T32 flyby from a hybrid simulation, *Ann. Geophys.*, *27*, 669–685, doi:10.5194/angeo-27-669-2009.

G. M. Chanteur, LPP-Ecole Polytechnique, 91128 Palaiseau Cedex, France.

E. Dubinin, MPS, Max-Planck-Str., 2, Lindau-Katlenburg D-37191, Germany.

R. Modolo, UVSQ/LATMOS-IPSL/CNRS-INSU, Quartier des Garennes, 11 bd d'Alembert, Guyancourt F-78280, France. (ronan.modolo@latmos.ipsl.fr)